University of Nebraska - Lincoln

DigitalCommons@University of Nebraska - Lincoln

U.S. Environmental Protection Agency Papers   U.S. Environmental Protection Agency

2012

Dose-Response Analysis of Bromate-Induced DNA Damage and Mutagenicity Is Consistent With Low-Dose Linear, Nonthreshold Processes

Maria A. Spassova
U.S. EPA, Spassova.maria@epa.gov

David J. Miller
NCEA

David A. Eastmond
University of California - Riverside

Nadejda S. Nikolova
Langley High School

Suryanarayana V. Vulimiri
NCEA

See next page for additional authors

Follow this and additional works at: https://digitalcommons.unl.edu/usepapers

Authors

Maria A. Spassova, David J. Miller, David A. Eastmond, Nadejda S. Nikolova, Suryanarayana V. Vulimiri, Jane Caldwell, Chao Chen, and Paul D. White

Research Article

Dose-Response Analysis of Bromate-Induced DNA Damage and Mutagenicity Is Consistent With Low-Dose Linear, Nonthreshold Processes

Maria A. Spassova,[1]* David J. Miller,[1] David A. Eastmond,[2]
Nadejda S. Nikolova,[3] Suryanarayana V. Vulimiri,[1] Jane Caldwell,[1]
Chao Chen,[1] and Paul D. White[1]

[1]National Center for Environmental Assessment (NCEA), Office of Research and Development (ORD), U.S. Environmental Protection Agency (U.S.EPA), Washington, DC
[2]Department of Cell Biology and Neuroscience, University of California, Riverside, California
[3]Langley High School, McLean, Virginia

Mutagenic agents have long been inferred to act through low-dose linear, nonthreshold processes. However, there is debate about this assumption, with various studies interpreting datasets as showing thresholds for DNA damage and mutation. We have applied rigorous statistical analyses to investigate the shape of dose-response relationships for a series of in vitro and in vivo genotoxicity studies using potassium bromate ($KBrO_3$), a water ozonation byproduct that is bioactivated to a reactive species causing oxidative damage to DNA. We analyzed studies of $KBrO_3$ genotoxicity where no-effect/threshold levels were reported as well as other representative datasets. In all cases, the data were consistent with low-dose linear models. In the majority of cases, the data were fit either by a linear (straight line) model or a model which was linear at low doses and showed a saturation-like downward curvature at high doses. Other datasets with apparent upward curvature were still adequately represented by models that were linear at low dose. Sensitivity analysis of datasets showing upward curvature revealed that both low-dose linear and nonlinear models provide adequate fits. Additionally, a simple biochemical model of selected key processes in bromate-induced DNA damage was developed and illustrated a situation where response for early primary events suggested an apparent threshold while downstream events were linear. Overall, the statistical analyses of DNA damage and mutations induced by $KBrO_3$ are consistent with a low-dose linear response and do not provide convincing evidence for the presence of a threshold. Environ. Mol. Mutagen. 00:000–000, 2012. © 2012 Wiley Periodicals, Inc.

Key words: dose-response; bromate; genotoxicity; reactive oxygen species; low-dose linearity

INTRODUCTION

Dose-response patterns for induction of mutations and other genotoxic effects induced by radiation and exogenous chemical agents have long been inferred to be linear [Ehling et al., 1983; Grosovsky and Little, 1985; Poirier and Beland, 1994; Frantz et al., 1995; Jansen et al., 1995].

The inference of a linear dose-response for mutagenesis has also served as support for inferring the likelihood of low-dose linearity in carcinogen risk assessment. U.S. EPA guidelines for carcinogen risk assessment recommend that a linear low-dose extrapolation approach be used for the risk assessment of carcinogens which are mutagens that

directly interact with DNA. Various other authoritative bodies such as the World Health Organization's Regional Office for Europe, the International Programme for Chemical Safety, the European Commission, and Health Canada have also incorporated information on genotoxicity into their carcinogen risk assessment guidelines [European Commission, 1996; Zeiss et al., 1999]. However, there has been debate in the scientific literature about the assumption of linearity in the action of mutagens [Henderson et al., 2000; Bolt et al., 2004; Pottenger and Gollapudi, 2009]. Various studies have interpreted experimental dose-response data as showing thresholds in the dose-response of DNA damage and mutation induced by genotoxic agents [Doak et al., 2007; Yamaguchi et al., 2008; Platel et al., 2009; Gocke et al., 2009; Seager et al., 2012]. However, rigorous statistical analyses of the dose-response dependence have not commonly been performed. Recent publications have applied statistical methods with a goal to identify a threshold point below which there is no response to a genotoxic agent (c.f. [Johnson et al., 2009; Lutz and Lutz, 2009; Seager et al., 2012]). Here we illustrate the use of an analytical approach to examine the shapes of dose-response relationships in experimental studies of mutagenesis and related measures of genotoxicity. In particular, we examine the consistency of these datasets with dose-response models that are low-dose linear. At the outset it is important to note that such low-dose linear models do not imply a fully linear (straight line) response over an entire experimental dataset. In particular, a variety of effects involving, for example, saturation of metabolic processes or occurrence of overt cellular toxicity may cause observed dose-response patterns to show upward or downward curvature at higher doses. Thus, the empirical question of interest here regards the shape of observed dose-response patterns at lower (but necessarily experimentally accessible) dose levels.

For this study, we focused on an example where genotoxicity is related to oxidative damage to DNA. We have examined datasets of mutagenic and related genotoxic effects of potassium bromate ($KBrO_3$), a carcinogen that induces oxidative damage to DNA and has been considered to likely have a genotoxic mode of action [IARC, 1999; Moore and Chen, 2006]. $KBrO_3$ was selected based on the multiple lines of evidence indicating that $KBrO_3$ and/or its metabolites directly interact with DNA residues to produce oxidative DNA damage [IARC, 1999; Arai et al., 2003; Ballmaier and Epe, 2006; Moore and Chen, 2006]. The damage is reported to occur following $KBrO_3$ bioactivation that involves cellular reductants such as glutathione (GSH) and produces an active intermediate. This unknown intermediate generates 8-hydroxy-2-deoxyguanosine (8-OH-dG) DNA adducts [Murata et al., 2001; Ballmaier and Epe, 2006]. This is considered the initiating step for further DNA alterations

including single-strand and double-strand DNA breaks (SSB and DSB), deletions and mutations. Based on this theory, extracellular and intracellular GSH concentrations may influence the dose-response dependence and inter-individual or animal variability. Note that analyses presented in this paper concentrate on the examination of available data on DNA damage and mutations induced by $KBrO_3$; an analysis of the mode (or modes) of action for $KBrO_3$ in the induction of cancer involves a variety of other scientific issues and is not addressed in this paper.

Numerous dose-response studies have been conducted on the genotoxicity and mutagenicity of $KBrO_3$ using acellular and cellular systems as well as experimental animals. It has been reported that at the molecular (cell-free) level, DNA damage by $KBrO_3$ follows linear dose-response dependence. For example, when bacteriophage PM2 DNA was used in a relaxation assay, DNA damage increased linearly with concentrations of $KBrO_3$ between 0.1 and 1 mM when incubated in the presence of glutathione (GSH) [Ballmaier and Epe, 1995; Ballmaier and Epe, 2006]. Similarly, using calf thymus DNA, Murata et al. [Murata et al., 2001] measured 8-OH-dG formed by $KBrO_3$ and its dependence on the presence of GSH and several other thiol-containing peptides. Their data also did not show any indication of sublinearity, when visually inspected. However, in cellular and whole animal systems there have been a variety of different results presented in the literature regarding the shape of dose-response dependence.

In this study we provide an organized statistical examination of dose-response patterns observed in experiments for a range of test systems examining DNA damage and mutagenesis by $KBrO_3$. As evident from the examples presented, a large number and variety of genotoxicity studies have been conducted for $KBrO_3$ in vitro and in vivo using a wide range of concentrations or doses. The objective of our study was to perform more formal and rigorous dose-response modeling of the $KBrO_3$ genotoxicity data with a particular emphasis on the types of damage believed to be most relevant to direct-acting oxidative mutagens. In particular, we wanted to examine the degree to which reported data were consistent with low-dose linear relationships, or, alternatively, were indicative of relationships showing either strong sublinear or supralinear patterns. We approached this evaluation by first identifying the studies for each of several important types of test systems that would best support statistical examination of the dose-response. Results of dose-response model fitting and graphical analysis are presented for each of these studies. Finally, we developed a simplified biochemical model to provide insight into how different biological processes can affect observed dose-response patterns. Biochemical modeling can illuminate differences in dose-response patterns that may be seen between early effects

Environmental and Molecular Mutagenesis. DOI 10.1002/em

Low-Dose Linearity of Bromate Genotoxicity   3

such as adduct formation and downstream processes such as single-strand DNA breakage.

METHODS

Study Selection

Prior to performing the dose-response analyses, an extensive review of the literature was conducted to identify studies that would be the most informative and relevant for dose-response modeling. We considered both in vitro and in vivo studies that measure $KBrO_3$ induced DNA damage using various genotoxicity assays. Examples from both categories were selected for further analyses based on the criteria described below. A table summarizing the studies that were considered is shown in the Appendix, Table AI. Studies were prioritized for subsequent analyses using scientific judgment generally based on the following considerations: (1) Higher priority was given to types of genetic damage such as 8-OH-dG adduct formation, DNA strand breakage, micronucleus formation and deletion mutations, which have been shown to be the most sensitive to oxidative mutagens [Moore and Chen, 2006; Luan et al., 2007]; (2) Results from experiments using mammalian cells in culture or those using laboratory animals (mice or rats) were favored over those conducted in acellular systems or using non-mammalian species; (3) Studies that used the widest range of test concentrations or administered doses were also given priority; (4) Studies that used the lowest doses, capable of revealing the shape of the dose-response at the low-dose region were given high priority; and (5) In vivo studies conducted using an oral route of exposure were generally preferred to those which used parenteral routes of administration. In selecting studies, we made an effort to include relevant publications where the authors had suggested that data indicate sublinear/threshold behavior. For each major class of genotoxic effect being considered, one, or occasionally two, representative studies were selected for detailed dose-response modeling.

Statistical Analysis

Dose-response analysis was carried out using EPA's benchmark dose software (BMDS) and original scripts in MATLAB. The results were plotted using MATLAB or Origin software. We used a likelihood approach to evaluate the dose-response models' goodness-of-fit. The likelihood was evaluated under the assumption of binomial, log-normal or normal distributions of the responses. As a general approach, we examined data to see if it was consistent with a simple linear (straight-line) relationship, where response was proportional to dose. In situations where the data indicated curvature in response, we used models consistent with the pattern of response observed. When data showed downward curvature suggestive of a plateauing of response, we examined the fit of Michaelis-Menten type models, exponential models [Slob, 2002] or a generalization of the Michaelis-Menten model (a bent-hyperbola model) as discussed further below. The bent-hyperbola model also allows for a fit of data that appear to have a ''change point'' between two linear segments of the dose-response. For data showing upward curvature or more complex patterns of response, we examined the fit of the bent-hyperbola model and models from an exponential family [Slob, 2002]. These exponential models have important features in that they describe various irreversible biological processes. Additionally, an exponential model can reflect data that show upward curvature at higher doses but may be consistent with a more linear response at low dose. We also conducted analyses examining the comparative fit of exponential models, quadratic models and hockey stick (threshold) model for datasets showing upwards curvature.

Mathematically, a low-dose linear relationship may be defined as one that has a positive slope extending down to the zero dose control group (slope > 0 at dose$=0$). For practical considerations it is also important to understand the magnitude of the estimated low dose response as compared with responses in the observed study range. To provide an indicator of the relative magnitude of the low dose slope, we have calculated the ratio of the slope at the lowest-observed-effect-level (LOEL) *divided by* the slope at zero. An index value of one would suggest a highly linear response in the low dose region (for doses extending up to the observed LOEL). On the other hand a large value of the index would indicate a low dose slope that is small in comparison with slopes at the LOEL. Finally a small value of the index would indicate a low dose slope that exceeds the slope at the LOEL. Here we were particularly concerned with data with upward curvature that might suggest a threshold, and we have used this slope index in interpreting modeling results for these datasets.

A goodness-of-fit p-value and the Akaike information criterion (AIC), a commonly employed statistical approach to allow comparison of fit across model types, were used to judge the appropriateness of the models. The AIC is defined as $-2L + 2p$, where L is the log-likelihood at the maximum likelihood estimates (MLE) for the model parameters, and p is the number of model parameters estimated. A likelihood-ratio test that compares the full model to each dose-response model was used to derive the goodness-of-fit p-values. The full model allowed the mean to vary independently across doses. We considered a model appropriate if the p-value was > 0.1. Unless otherwise noted, the data are plotted with their 95% confidence limits.

Cell culture data were tested by binomial dispersion test to define the homogeneity between replicas where applicable. Binomial dispersion test was performed after Richardson et al. [1989] with test statistics:

$$\mathbf{X}^2 = \sum_{i=0}^{d} \sum_{j=1}^{r_i} \frac{(z_{ij} - k_{ij}\hat{p}_i)^2}{k_{ij}\hat{p}_i(1 - \hat{p}_i)}, \tag{1}$$

where d is the number of doses, with $i = 0$ being the control, r_i is the number of replicates in the ith dose, p_i is the proportion of aberrant cells in the ith dose group (number of aberrant cells summed over the replicate cultures exposed to dose i divided by the total number of cells sampled at dose i), k_{ij} is the number of cells sampled from the jth replicate culture exposed to dose i, among which the number of aberrant cells was z_{ij}. The test statistics was compared to a χ^2 distribution with $\sum_{i=0}^{d}(r_i - 1)$ degrees of freedom.

In one analysis, the test revealed significant underdispersion in a data set [Platel et al., 2009], with p-value < 0.001. To properly model the responses distribution we used a generalization of the binomial distribution capable of modeling underdispersed data. More specifically, the multiplicative binomial (mB) distribution [Altham, 1978] was used to analyze the data from Platel et al. [2009]:

$$\Pr(Z_k = j) = \binom{k}{j} p^j q^{k-j} \theta^{j(k-j)} / f(p, \theta, k), \quad o \leq j \leq k$$

$$f(p, \theta, k) = \sum_{j=0}^{k} \binom{k}{j} p^j q^{k-j} \theta^{j(k-j)} \tag{2}$$

The mB distribution contains an additional parameter $\theta > 0$ as compared to the binomial distribution [Eq. (2)] and allows for modeling of overdispersed ($\theta < 1$) or underdispersed ($\theta > 1$) data, where $0 < P = 1-q < 1$. The indices have their usual meaning for binomial distribution – k is the sample size and j is the number of successes. Z_k here is a random variable that represents the number of aberrant cells out of k cells. More specifically Z_k is the sum of random variables $X_1,\ldots, X_k$, which represent the response of each cell with possible values 0 (normal) and 1 (aberrant). The assumption for derivation of the multiplicative binomial

Environmental and Molecular Mutagenesis. DOI 10.1002/em

4   Spassova et al.

distribution is that $X_1, \ldots, X_k$ are identically distributed but not independent variables with symmetric joint distribution and no second- or higher-order interactions (no three-variable interaction). To apply the model for dose-response data we assumed that θ is dose independent.

To model dose-response shapes that showed saturation that was not well fit by a Michaelis-Menten model or where there was an apparent change point between two linear slopes, we used a generalization of the Michaelis-Menten model (gMM) also known as bent-hyperbola model [Ridout, 1994]. To fit data showing saturation, the model was modified to have a horizontal positive asymptote as follows:

$$E[y|x] = \theta_0 + \theta_1(x - \alpha) - \theta_1\sqrt{(x-\alpha)^2 + \gamma} \qquad (3)$$

This modified model has low-dose linear properties and saturates at high doses. Furthermore the model allows for more flexible transition to saturation (either faster or slower) compared with the classical Michaelis-Menten model.
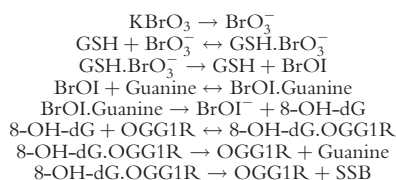
The bent-hyperbola model can also be modified to a hockey stick model with a horizontal negative asymptote and a sharp bend between the two slopes:

$$E[y|x] = \theta_0 + \theta_1(x - \alpha) + \theta_1\sqrt{(x-\alpha)^2 + \gamma}, \qquad (4)$$

where $\sqrt{\gamma} = 10^{-6}$. The specification of this small fixed value of γ causes the hyperbola to have a very tight ''change point'' (bend) and represent a hockey stick model. This threshold model was used to fit the data from Seager et al., 2012 and compare their AIC values to that of the low-dose linear nonthreshold model.

Biochemical Kinetic Model

The biochemical model developed here contains elements reflecting a series of processes involved in DNA damage by bromate: interaction with a biomolecule (here represented by GSH) to form a DNA reactive species, production of DNA adducts, and the presence of a repair process that removes adducts. This repair process can also result in error leading to production of strand breaks, although at a much lower rate than successful repairs. This model is not intended to be predictive of rates of DNA damage in vivo or in vitro, as the current understanding of the processes involved is insufficient to support a predictive model. Rather, the model is intended to support further quantitative understanding of how different processes involved in this system can interact and how this may influence shapes of dose-response relationships. The biochemical model contains a series of bromate- and oxygen-derived molecules that participate in the following eight chemical reactions:

$$\begin{aligned} KBrO_3 &\rightarrow BrO_3^- \\ GSH + BrO_3^- &\leftrightarrow GSH.BrO_3^- \\ GSH.BrO_3^- &\rightarrow GSH + BrOI \\ BrOI + Guanine &\leftrightarrow BrOI.Guanine \\ BrOI.Guanine &\rightarrow BrOI^- + 8\text{-}OH\text{-}dG \\ 8\text{-}OH\text{-}dG + OGG1R &\leftrightarrow 8\text{-}OH\text{-}dG.OGG1R \\ 8\text{-}OH\text{-}dG.OGG1R &\rightarrow OGG1R + Guanine \\ 8\text{-}OH\text{-}dG.OGG1R &\rightarrow OGG1R + SSB \end{aligned}$$

where the dot notation signifies a bound complex of two participants. Some of these reactions are based on those proposed by Kawanishi and Murata [2006]. Via interaction with reduced glutathione (GSH), an intermediate product (BrOI) is formed, which can form the oxidative lesion 8-OH-dG on DNA. These lesions can subsequently be repaired by an appropriate repair mechanism (which we label OGG1R), or alternatively a single strand break can persist due to a failed repair attempt. The model elements Guanine, GSH, and OGG1R were given appropriate initial values and $KBrO_3$ was dosed at time zero. The reactions were modeled using simple mass-action kinetics, with all simulations carried out using MATLAB SimBiology software. In the absence of repair, OGG1R binding rates were set to zero.

RESULTS AND DISCUSSION

In Vitro Studies

Following the initial screen and study selection, we used dose-response modeling to analyze the data from four studies conducted to investigate the genotoxic and mutagenic effects of $KBrO_3$ in mammalian cell culture systems. First, we focused on a recently reported $KBrO_3$ genotoxicity study, where the results were interpreted by the authors as showing a threshold [Platel et al., 2009]. As described in the study report, TK6 human lymphoblastoid cells were exposed to various concentrations of $KBrO_3$ between 6.25 μM to 5 mM for 1 to 24 h, and the cells were harvested for the micronucleus test 24 hr after the beginning of exposure.

A binomial dispersion test [Richardson et al., 1989] was used on the experimental replicates to determine if the responses followed a binomial distribution. The test revealed no overdispersion. Instead, underdispersion was encountered as compared with the expected binomial distribution dispersion, with P-value = 0.001 (see Methods). Underdispersion might reflect some type of cell–cell interaction in the cell suspension or could be a result of a procedural matter that was not apparent to us in this review. To appropriately analyze the data, we used a generalized binomial distribution named multiplicative binomial (mB) [Altham, 1978]. While the response's distribution was modeled with mB, the concentration dependence of the responses was modeled with a linear function for the data from the experiments using the 1, 2, and 3 hr periods of exposure (Figs. 1A–1C).

We used a likelihood approach to test the appropriateness of the model. The likelihood of the model was compared to a full model in a likelihood ratio test (goodness-of-fit test). The high goodness-of-fit P-values for this test, between 0.38 and 0.92, suggest that a linear model is highly appropriate (Figs. 1A–1C). In contrast, the data from 24 hr of exposure (Fig. 1D) showed some clear saturation of the response at high concentrations. After determining that a Michaelis-Menten model in BMDS (dichotomous Hill with slope = 1) did not provide an adequate fit, we modeled these using a generalization of the Michaelis-Menten model (gMM) also known as the bent-hyperbola model [Ridout, 1994]. The model was modified to have zero slope of the positive asymptote (Eq. 3). As before, a likelihood-ratio test was used to define the appropriateness of the model and gave $P = 0.95$, indicating that the model is highly consistent with the data.

The dose-response analysis of the data reveals high consistency with low-dose linear models and thus is not
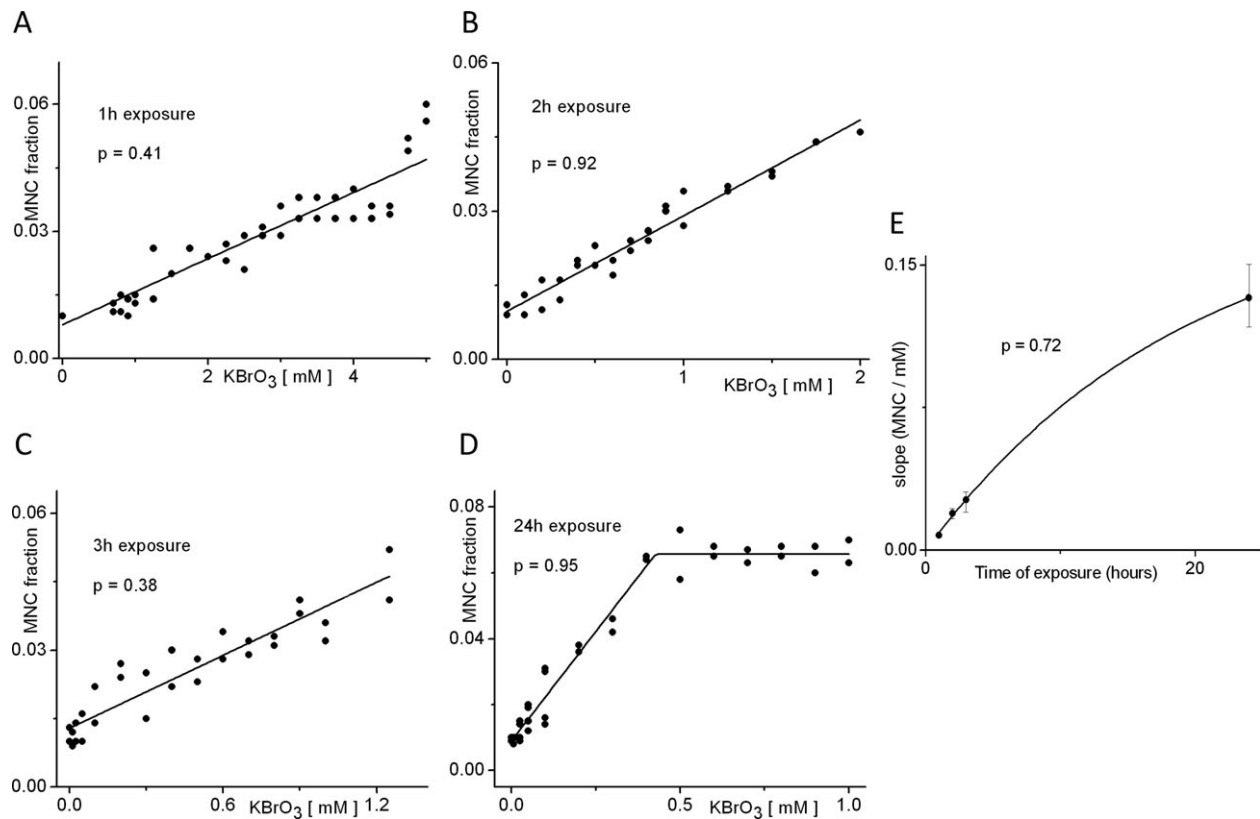
Environmental and Molecular Mutagenesis. DOI 10.1002/em

Low–Dose Linearity of Bromate Genotoxicity   5

Fig. 1. DNA damage in TK6 human B-lymphoblastoid cells measured using the micronucleus assay. **A–D:** Micronucleated cells (MNC) formed at various concentrations and times of exposure to $KBrO_3$ based on data from Platel et al. are shown [Platel et al., 2009]. The data were assumed to follow a generalized binomial distribution [Altham, 1978] that allows for modeling underdispersed data (see text). A likelihood approach was used for the statistical analysis. **A–C:** A linear model was fit to the three sets of data at the low exposure times (1, 2, and 3 hr). **D:** A generalization of Michaelis-Menten equation [Ridout, 1994], also known as a bent-hyperbola model, was used to model the data following the 24-hr exposure that shows saturation at high doses. This model retains the low dose linear behavior of the Michaelis-Menten model, but allows for data-dependent curvature to predict more rapid saturation as compared to the Michaelis-Menten model. The goodness-of-fit P-values are indicated for each dataset and show a high adequacy of the models. **E:** The slope parameter MNC/$[KBrO_3]$ from A–D, is plotted vs. time of exposure. For D, approximation of the slope was defined from θ_1 (Eq.2) as in this case $\alpha^2 \gg \gamma$. The 90% confidence intervals defined by the profile-likelihood method [Crump and Howe, 1985] are shown as error bars. The time dependence was fit with an exponential model [Slob, 2002]. The model predicts maximal potency MNC/$[KBrO_3]$ of 0.19 (see text).

indicative of a threshold for this response. In addition, the data from this study allowed us to analyze the potency of unit concentration of $KBrO_3$ to induce micronucleated cells (MNC) as a function of time (MNC/$[KBrO_3]$ vs. time of exposure, Fig. 1E). Such analysis can allow us to define the maximal potency of $KBrO_3$ as a measure of the full clastogenic potency of this chemical. For the 24 hours exposure data modeled by the gMM model, we used the slope at the low dose region to define MNC/$[KBrO_3]$ (Fig. 1D). As the gMM model parameter α^2 was much larger than γ ($\alpha^2 \gg \gamma$) at its MLE, the slope in the low dose region was approximately defined by θ_1 (Eq. 3). The time dependence of MNC/$[KBrO_3]$ is plotted on Figure 1E. While a linear model did not fit the data, an exponential model was fit to the data with high goodness-of-fit (p = 0.72). The maximal potency MNC/$[KBrO_3]$ was predicted by the model as 0.19, $\sim$ 50% higher than the experimental maximum. This value could be a useful char-

acteristic for comparing the genotoxicity of different chemicals.

A recent study on oxidative stress-induced genotoxicity was designed to examine the low dose responses to several chemicals, including $KBrO_3$, in the human B-lymphoblastoid AHH-1 cell line. An *HPRT* forward mutation assay and a cytokinesis-block micronucleus assay were performed [Seager et al., 2012]. These authors analyzed their data using a hockey stick model [Lutz and Lutz, 2009] and reported threshold estimates for the $KBrO_3$ data from both assays with a positive lower bound estimate for the threshold. When the lower bound of the threshold is positive, it provides statistical evidence that the threshold model is better than a perfectly linear model [Crump, 2011]. We reanalyzed the data from these experiments using continuous dose-response models (as discussed in Methods) and examined the goodness-of-fit of the models to the data. Our analysis indicated that the
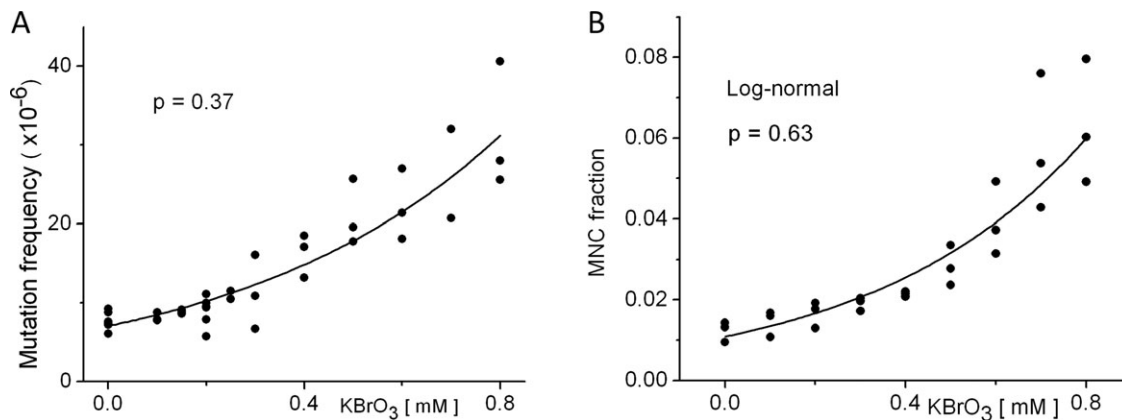
Environmental and Molecular Mutagenesis. DOI 10.1002/em

6   Spassova et al.

Fig. 2. KBrO$_3$ induced DNA damage in lymphoblastoid AHH-1 cell culture measured by HPRT forward mutation assay and cytokinesis-block micronucleus assay [Seager et al., 2012]. **A:** HPRT mutation frequency was quantified after exposure to various concentrations of KBrO$_3$ for 24 h. The data were fit with exponential dose-response model ([Slob, 2002], model 2) with power model of the variance that provided adequate fit with a goodness-of-fit p-value of 0.37. **B:** Micronucleus assay data from 24-hr exposure to KBrO$_3$ at various concentrations are plotted. Log-normal distribution of the responses was assumed and an exponential model ([Slob, 2002], model 2) with low dose linear properties was fit to the data with high goodness-of-fit $P = 0.63$ value.

data on the *HPRT* mutations are also consistent with an exponential low-dose linear model ([Slob, 2002], model 2) with a p = 0.37 (Fig. 2A). The data from the MN assay in the same study showed high overdispersion in the high dose region and were overdispersed overall. Therefore, models where the variance is estimated from the data were considered. As the MNC frequency was low, skewness of the data distribution was assumed and a log-normal distribution was used to represent the observed variability. The fully linear dose-response model did not provide an adequate fit for the MN data, consistent with the original analysis by Seager et al. [2012]. Upon further examination, we found that the data were well fit by an exponential model ([Slob, 2002], model 2) that is linear at low dose. The goodness-of-fit p-value of 0.63 indicates that the data are highly consistent with the exponential model (Fig. 2B). To compare the exponential model fits with the original analysis by Seager et al. [2012], we computed the AIC value for the hockey stick model fits (see Methods) and the exponential model fits. We used constant variance for both models as it is analogous to the least square fit procedure used by Seager et al. [2012]. The use of this approach did confirm the threshold values reported by Seager et al. [2012] as the MLE of the hockey stick model. The analysis of the HPRT data with the hockey stick model and the exponential model both provided an AIC value of 139, indicating that the data do not support one model over the other. Similarly, for the MN data, the hockey stick model gave an AIC value of 19, while the exponential model provided a lower but close AIC value of 17.

Another study investigated KBrO$_3$ induced DNA damage in TK6 cell cultures using the comet assay (COM) and MN test [Luan et al., 2007]. Visual inspection of the MN dose-response data in this study showed close to lin-

ear dependence with some suggestion of supralinearity at low doses. These data are consistent with our analysis of the Platel et al. data that supports low-dose linear dependence [Platel et al., 2009]. However, the COM assay data provided some suggestion of sublinearity, with the mean response of the first dose being numerically below the control level. We analyzed the dataset from the alkaline COM assay to test if it was consistent with a linear dose-response model. The neutral COM assay data presented some more pronounced nonmonotonic behavior that needs further investigation and we did not further analyze that data. A linear model with variance as a power function of the response fit the alkaline COM data with high goodness-of-fit value p = 0.72 (Fig. 3A), showing that a linear model appropriately represented this dataset. Here we want to clarify again that the consistency of the data with low-dose linear models does not definitively address the question of whether a biological threshold in response exists. We would note that this data set, given the spacing of the experimental doses and the observed variances, has little power to discern the nature of the dose-response relationship below the 1 mM concentration.

The genotoxic potency of KBrO$_3$ has also been investigated using a mouse lymphoma assay which measures mutations affecting the thymidine kinase (*Tk*) gene in L5178Y/*Tk*$^{+/-}$ cells. This assay is widely used due to its ability to detect both point and chromosomal mutations. In a study by Harrington-Brock et al. [2003], the dose-response of *Tk* mutations induced by KBrO$_3$ was determined. We used the data from this study to model the mutation frequency induced by KBrO$_3$. We assumed a normal distribution of the response with variance estimated from the data. In this dataset, the responses at the highest dose levels indicated a greater than linearly proportional response. The dose-response was successfully fit
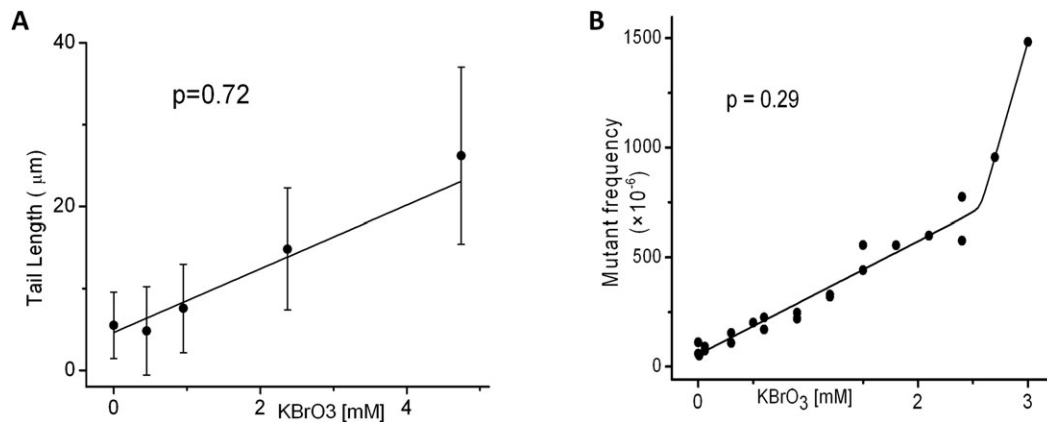
Environmental and Molecular Mutagenesis. DOI 10.1002/em

Low-Dose Linearity of Bromate Genotoxicity   7

Fig. 3. KBrO$_3$ induced DNA damage in cell cultures measured by comet assay and *Tk* mutant frequency. **A:** Alkaline comet assay as a measure of DNA damage was performed on TK6 cells treated with KBrO$_3$ for 4 hr. The data were reproduced from Luan et al. [Luan et al., 2007]. Linear model with modeled variance (BMDS) was fit to the data with a goodness-of-fit *P*-value = 0.72. **B:** *Tk* mutant frequency of L5178Y/*Tk*$^{+/-}$

mouse lymphoma cells after 4 hr. incubation with KBrO$_3$ [Harrington-Brock et al., 2003]. As regression analysis did not reveal significant differences between the two experiments, we analyzed the combined data from the two experiments, using a normality assumption, where the variance was estimated from the data. The dose-response was modeled with a bent-hyperbola model that yielded a *P*-value of 0.29.

by a bent-hyperbola model which fit the data with an acceptable level of likelihood compared to the full model with P = 0.29 (Fig. 3B). The low-dose linearity index (see methods) was 1 in this case. Once again, low-dose linearity was highly consistent with the data according to our statistical modeling.

In Vivo Studies

Further, we were interested in the dose-response shape of the DNA damage caused by KBrO$_3$ in vivo. Allen et al. [2000] used B6C3F1 male mice treated with KBrO$_3$ in drinking water at doses ranging from 0.08 to 0.8 g/L for 8 or 78 weeks. The rates of MN induction were determined in peripheral blood normochromatic and polychromatic erythrocytes (NCE and PCE, respectively). None of the four datasets, for two different treatment times and two different cell types, showed signs of sublinearity in the dose-response dependence, except possibly in the case of the MN in the PCEs after 78 weeks of exposure. The responses showed low frequency of the MN (maximum 6/1,000), a circumstance that can lead to a suggestion of some skewness of the distribution of the response. Therefore, we assumed a log-normal distribution of the responses. We analyzed the MN-NCE after 78 weeks of exposure. We chose the NCE for the analysis as they reflect more persistent KBrO$_3$ effects. A Michaelis-Menten model (linear at low dose and saturating at high doses) was used to fit the dose dependence of the MN-NCE after 78 weeks of exposure to allow for observed downward curvature at the higher doses in this dataset. The Michaelis-Menten model gave a goodness-of-fit *P*-value of 0.11, which indicates the model is consistent with the data (Fig. 4A). Another similar study performed by Awogi et al. [1992] examined peripheral blood PCE

for MN formation after in vivo exposure to KBrO$_3$. CD-1 male mice were dosed by single intraperitoneal injections administering KBrO$_3$ at doses ranging from 18.8 to 212 mg/kg [Awogi et al., 1992]. Blood was collected 0–96 hr after injection of KBrO$_3$. Two independent studies, by Nippon Glaxo, Tokyo Research (NGTR) and Otsuka Pharmaceutical Factory (OPF), are summarized in the article. We chose to model the OPF study data as it included an additional lower dose. We used the data from samples collected 24 hr after exposure, as they were collected at a commonly used time point for the MN test. Similar increases in MN were also seen at the 48 hr sampling period. There was a decrease in the response at the highest dose (212 mg/kg) at 24 hr, and so this data point was not used in the analysis. Again a log-normal distribution of the responses was assumed for reasons similar to those described earlier. We modeled the dose-response with an exponential model ([Slob, 2002], Model 4), another model which exhibits low-dose linear behavior. The goodness-of-fit *P*-value of 0.81 revealed that the model was highly consistent with the data (Fig. 4B). Based on our analysis and the overall review of the data, we conclude that in vivo genotoxicity of KBrO$_3$ in the bone marrow is consistent with linear behavior across the range of doses tested.

To address another important aspect in characterizing genotoxicity, we investigated the shape of the dose-response in one of the target organs, where tumor development has been detected. After careful review of the literature, we selected a study investigating genotoxicity in rat kidney cells after KBrO$_3$ exposure. The study had the most extended dose range toward low doses and a significant response was only observed at the high dose point of 500 ppm KBrO$_3$ in drinking water, leading the authors to suggest the existence of a no-effect level [Yamaguchi
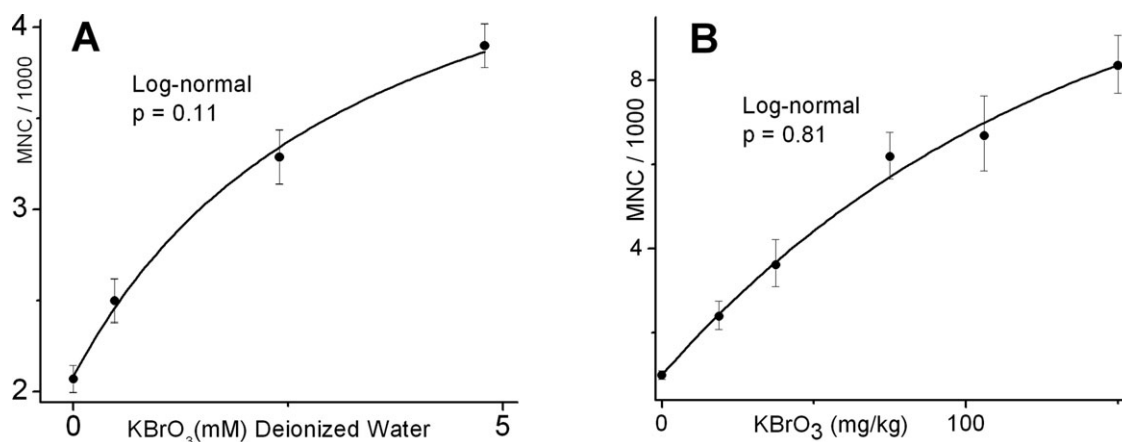
Fig. 4. Micronucleus (MN) induction by KBrO$_3$ in mice blood cells in vivo. Log-normal distribution was assumed for these data. The geometric mean responses with the 95% CI are plotted vs. KBrO$_3$ concentration. **A:** Effects of chronic (78 weeks) exposure to KBrO$_3$ in drinking water of B6C3F1 mice [Allen et al., 2000]. Data on peripheral blood normochromatic erythrocytes have been fitted with a Michaelis-Menten model. **B:** Micronucleus test results from the peripheral blood polychromatic erythrocytes of CD-1 male mice dosed with KBrO$_3$ (mg/kg) by intraperitoneal injection [Awogi et al., 1992]. The blood was collected 24 hr after the KBrO$_3$ injection. The dose-response has been modeled with an exponential model ([Slob, 2002], Model 4). The P-value of 0.81 reveals that the model is highly consistent with the data.

et al., 2008]. Furthermore, Yamaguchi et al. [2008] employed the NaI DNA isolation method with deferoxamine mesylate as a chelating agent. Such an approach should minimize the artifactual formation of 8-OH-dG during DNA isolation. Big Blue rats were treated for 16 weeks with KBrO$_3$ dissolved in their drinking water at concentrations between 0.02 and 500 ppm. Kidney genotoxicity was assessed by quantifying 8-OH-dG DNA adducts in kidney cells and point mutations, including GC->TA in the *lacI* gene of the transgenic rats. 8-OH-dG is considered to be the primary form of DNA damage by KBrO$_3$. However, because GC->TA transversion mutations have not been directly associated with 8-OH-dG frequency [Nakajima et al., 2002; Arai et al., 2003], we focused our analysis on the dose-response data of 8-OH-dG. These data were adequately fit with a linear (straight line) dose-response with P-value = 0.15 (not shown). We performed sensitivity analysis to examine the ability of these data to distinguish between different dose-response models. As the plot indicates some upward curvature, an exponential model was fit to the data (Fig. 5A). The goodness-of-fit test gave P = 0.23, which indicates that the model appropriately describes the data. The low-dose linear properties of this model are apparent on the inset of Figure 5A. Because of the wide range of doses employed, a semi-logarithmic plot (Fig. 5B) is also shown to reveal visually the goodness-of-fit. Note however, that frequently used semi-logarithmic plots give distorted impressions of the dose-response shapes, as even a straight line will appear to have upward curvature when so plotted. Given that these data suggest an upward curving response, we also fit a quadratic model with no linear term to the data (Fig. 5C). This model also fit the data appropriately (goodness-of-fit p = 0.35). To further compare different models we used the AIC that is based on the likelihood values, but also penalizes for each additional model parameter. The three models (linear, exponential and quadratic) had sufficiently close AIC values of −100, −112, and −114, respectively. Overall, statistical modeling showed that this dataset had little power to resolve the shape of the underlying dose-response relationship and could be fit with models that were linear as well as models that were nonlinear at low dose.

The process of DNA damage by KBrO$_3$ is believed to start with generation of 8-OH-dG DNA adducts, though some evidence suggest that SSBs can be generated directly by KBrO$_3$ under cell-free conditions [Ballmaier and Epe, 2006]. The 8-OH-dG adducts are repaired by a base-excision repair (BER) mechanism, where the first step is the adduct's excision by 8-oxoguanine DNA glycosylase (Ogg1). At this point, a single-strand break (SSB) is created. In some cases further repair might fail and result in an accumulation of SSBs. Large deletion mutations can arise from double strand breaks (DSBs) or adjacent SSB, and it has been demonstrated that this type of mutation accounts for 90% of the mutations induced by KBrO$_3$ in TK6 lymphoblastoid cells [Luan et al., 2007]. Accordingly, large deletion mutations are considered to be a major mode of KBrO$_3$ genotoxicity. We therefore considered DNA deletions in the kidney, a target organ, to be an important end point. We investigated the dose-response relationship of KBrO$_3$-induced deletion mutations in kidney cells using a study by Umemura et al. [2006] in which the authors measured the Spi$^-$ deletion mutation frequency in the kidneys of *gpt* delta rats exposed to KBrO$_3$. KBrO$_3$ was added to the drinking water at concentrations between 60 and 500 ppm for 13 weeks. Again, we were interested to find if low-dose
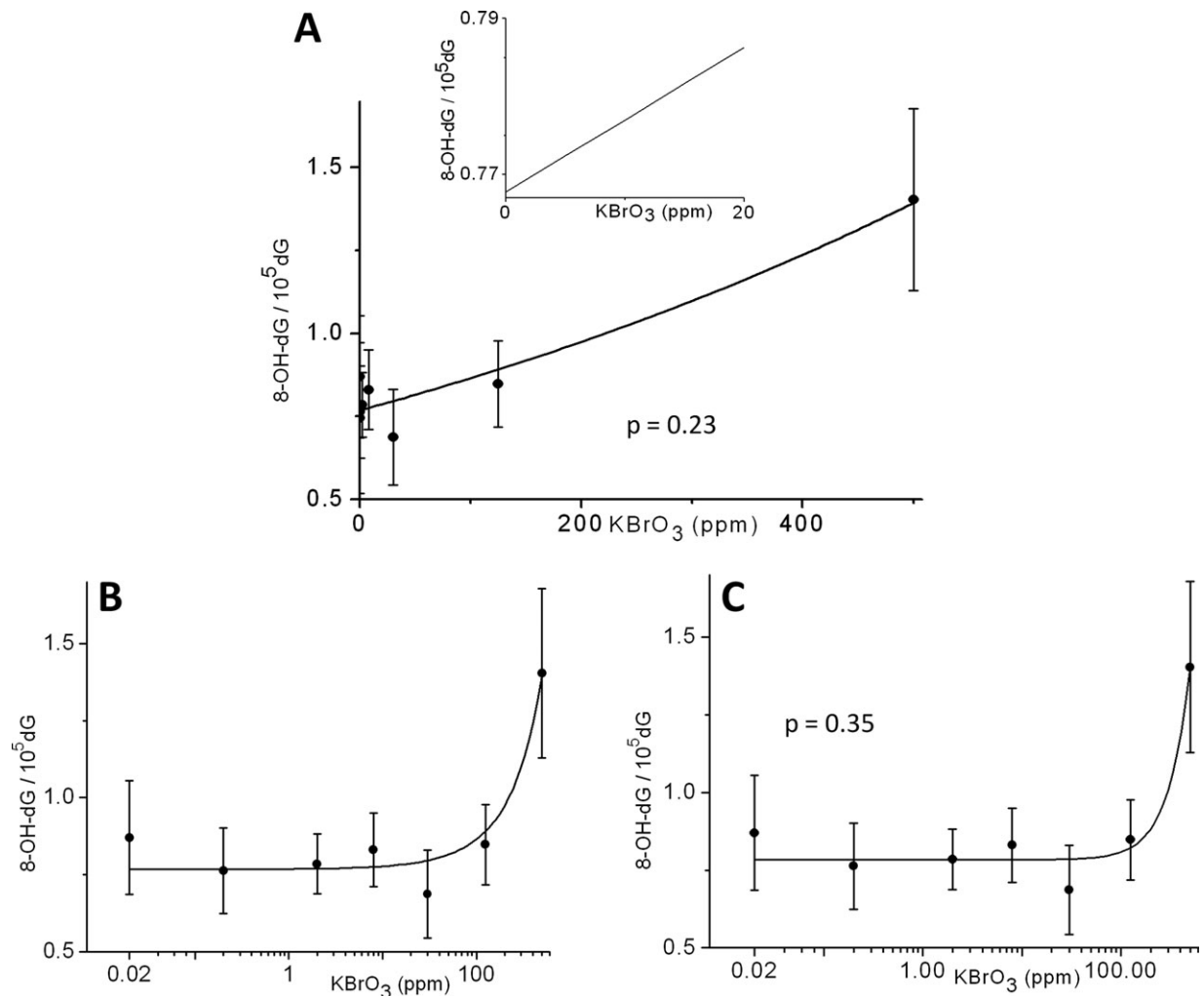
Environmental and Molecular Mutagenesis. DOI 10.1002/em

Low-Dose Linearity of Bromate Genotoxicity   9

Fig. 5. Dose-response dependence of DNA oxidation in the kidney, a target organ of $KBrO_3$ carcinogenesis. Big Blue rats were exposed to $KBrO_3$ added to their drinking water for 16 weeks. Data on 8-OH-dG/ 10^5 dG bases of DNA extracted from the kidneys [Yamaguchi et al., 2008] are plotted vs. $KBrO_3$ concentration. We analyzed the data using two models: (1) low-dose linear model and (2) a model with zero slope at zero dose. We used an exponential model ([Slob, 2002], Model 2) with low-dose linear behavior (**A–B**) and a quadratic model with a zeroed linear term (**C**), respectively. The exponential model is presented in linear coordinates in **A.** The low-dose dependence (A inset) is indistinguishable from linear. The data are plotted on a semilogarithmic scale (**B–C**) to reveal visually similar goodness-of-fit of both exponential and quadratic models. Both models adequately fitted the data with close Akaike information criterion (AIC) values of −114 and −112 respectively, indicating that the actual shape of the dose-response curve cannot be resolved from the existing data.

linear models can give appropriate fit to the data. As these data were not adequately fit by linear (straight line) models in BMDS and the plot indicated some upward curvature, an exponential model ([Slob, 2002], model 2) with low-dose linear properties was fit to the data (Fig. 6). A log-normal distribution of the response gave an improved fit to the data with a goodness-of-fit P-value $P = 0.11$. The appropriate fit of the model also indicates that for this important end point low-dose linearity is consistent with the data.

Using $KBrO_3$ as an example, we investigated the shape of the dose-response for a number of genotoxicity and mutagenicity endpoints across multiple studies. Specifi-

cally, we were interested in determining if linearity at low doses is a common feature of the dose-response relationships for this agent that acts directly and/or through its metabolites to induce oxidative damage to DNA. $KBrO_3$ was selected as a genotoxic agent that repeatedly has been shown to be carcinogenic in male and female rats, and is probably carcinogenic in mice and hamsters [Kurokawa et al., 1990; DeAngelo et al., 1998; IARC, 1999]. Our analysis of different endpoints at the cellular and organismal levels showed overall consistency with low-dose linear models. We found that each data set we examined could be appropriately fit by models that have linear behavior at low dose. Low-dose linear models
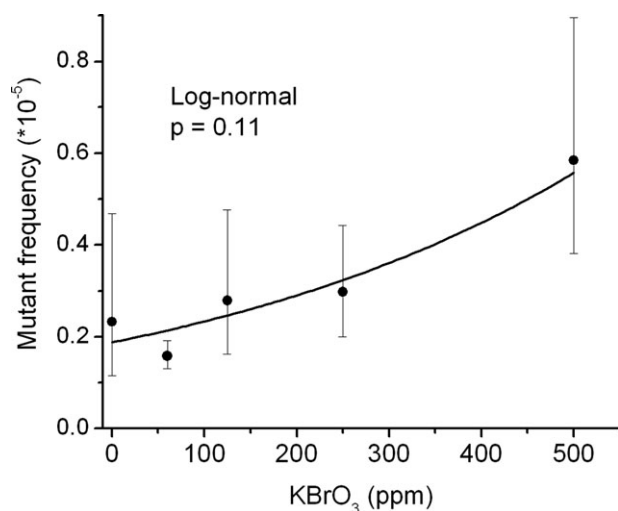
Environmental and Molecular Mutagenesis. DOI 10.1002/em

10   Spassova et al.

Fig. 6. Deletion mutations in the kidneys of gpt delta rats exposed to KBrO₃. Dose-response data from Umemura [2006] are plotted. An exponential, low-dose linear, model ([Slob, 2002], model 2) is fit to the data for Spi⁻ mutation frequency as a measure of deletion mutations. A log-normal distribution of the data at each concentration was assumed and a log-scale constant variance model was used.

fit all the datasets with a P > 0.1, which is even more conservative measure than the P = 0.05 value commonly used as a cutoff for statistical significance. In these analyses, a value lower than the p-value cutoff would suggest that the model is not consistent with the data. In the majority of cases examined, we found that the data were fit either by a linear (straight line) model or a relationship which is linear at low dose and shows a saturation-like downward curvature at high dose. These data included micronucleus results in TK6 human B-lymphoblastoid cells *in vitro* as well as MN induction in mice blood cells in vivo. In other datasets, some degree of upward curvature was present in the data which was reflected in the statistical modeling. However in these cases, the data were still appropriately represented by models having low-dose linear behavior. The low-dose linearity index for all of these datasets was below 3. These data included mutation and MNC frequency in AHH-1 human B-lymphoblastoid cells, mutant frequency in L5178Y/*Tk*+/- mouse lymphoma cells and deletion mutations in the kidneys of *gpt* delta rats. It is important to recognize that, in some cases, statistical fitting of assay data can have limited power to determine dose-response relationships. We examined this issue in modeling the data on 8-OH-dG kidney adduct levels in Big Blue rats. We found that an alternative nonlinear model – a quadratic model with no linear term – also provided an appropriate fit to the data, indicating that these data had little power to resolve the shape of the underlying dose-response relationship. Furthermore, the data on mutation and MNC frequency in AHH-1 cells were also consistent with both, threshold and low-dose linear models. As noted in the introduction,

our analyses were focused on examining the substantial database relevant to dose-response patterns for the genotoxic effects of KBrO3; we have not undertaken evaluation of all the data and scientific issues that would be included in a mode of action analysis for KBrO₃ carcinogenicity.

As shown in the Appendix, Table A1, the generation of 8-OH-dG adducts is a common endpoint measured in cell-free, in vitro cell culture and in vivo conditions. As it is considered a primary effect of KBrO₃ exposure, this end point might be a good anchor for comparison of the in vitro vs. in vivo effects of KBrO₃; acute vs. continuous exposure; and rat vs. human exposure. For purposes of this article, measurements of this endpoint allow some comparison of the effective cellular doses of KBrO₃ between in vivo and in vitro conditions. For example in two early studies by the same group [Sai et al., 1992, 1994] using the same species (male F344 rats), both in vivo and in vitro experiments were performed. The increase in 8-OH-dG in the kidney after a single in vivo exposure to 80 mg/kg KBrO₃ by intraperitoneal injection (48 hr after treatment) was comparable with the increase of 8-OH-dG observed in an in vitro preparation of kidney proximal tubules exposed to 5 mM KBrO₃ for 4 hr (Appendix, Table A1). Although such comparisons can give some guidance for extrapolation from one type of study to another, consistency among studies and potential differences in bioactivation are important factors to be considered. It is important to note that in some earlier studies the background levels of 8-OH-dG might be elevated artifactually during DNA isolation and enzymatic digestion. Also it is important to account for possible saturation at high doses, in which case, the lowest dose that produces the maximal effect can be used in making comparisons.

As a tool to provide insight into different factors that may affect the observed shapes of dose-response relationships, we also developed a biochemical kinetic model of KBrO₃-induced DNA damage (Fig. 7). We did not attempt to incorporate all available biological information in our model, but to develop a simplified model that illustrates a basic phenomenon. We were interested to study the possible dose-response shapes of downstream events, when an upstream event has a sublinear shape. This is an important question to be investigated, as in some cases the presence of a nonlinearity or apparent threshold in an early upstream event is used as a reason to conclude that downstream events also have a threshold. For this purpose not all biochemical reactions are represented in detail in the model and in some cases a reaction in the model includes several biochemical steps. In our model, KBrO₃ can interact reversibly with GSH to form reactive oxygen intermediates (BrOI) that can directly cause oxidative DNA damage (Fig. 7A). Even though some evidence suggests that BrOI can directly generate SSB [Ballmaier and Epe, 1995; Ballmaier and Epe, 2006], we only considered
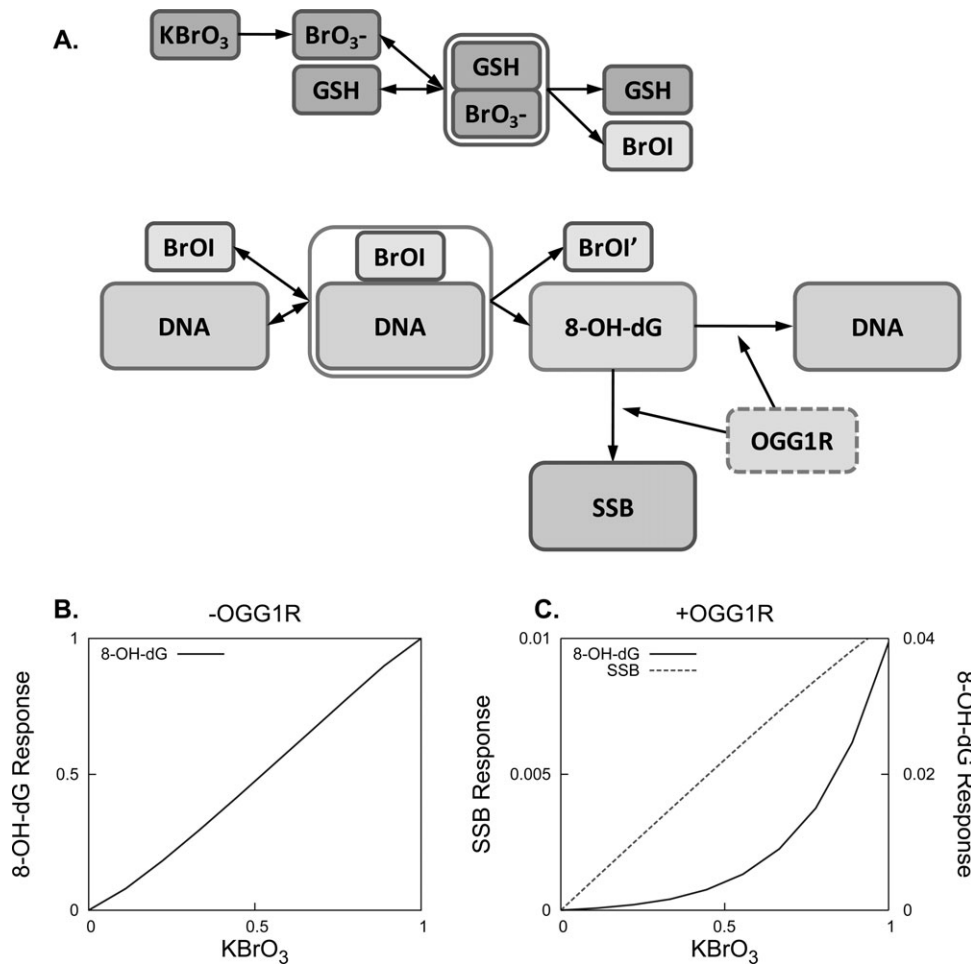
Environmental and Molecular Mutagenesis. DOI 10.1002/em

Low–Dose Linearity of Bromate Genotoxicity 11

Fig. 7. KBrO$_3$ – DNA damage mechanism. **A:** The model depicts a process of DNA damage, where the initial step is dG base oxidation by a KBrO$_3$-GSH interaction intermediate product (BrOI). (**B** and **C**) Simulation based on the model in (**A**) with base-excision repair mechanism initiated by Ogg1 (OGG1R) included in the model simulation presented in (**C**) but not in (**B**). The simulation responses are normalized by the maximum adducts observed in absence of repair within the dose range explored. In (**B**), the dose-response curve is shown for the formation of 8-OH-dG adducts in the absence of an effective base-excision repair mechanism (-OGG1R). In (**C**), SSB are generated subsequent to the DNA oxidation as a byproduct of an unsuccessful DNA repair (see text). In such a scenario, the 8-OH-dG is increasingly repaired with time after exposure, while SSB continuously accumulate. Dose-response curves are shown for both adducts (solid line) and single strand breaks (dashed line) in the presence of repair. The dose-response profiles for 8-OH-dG and SSB were computed at a time point after the KBrO$_3$ exposure, shortly before the steady state is reached. The figure demonstrates that even if an upstream endpoint (8-OH-dG) might present with sublinear/threshold like dose-response dependence, a downstream process of SSB generation can have linear dose-response dependence. Note the difference in scales for 8-OH-dG and SSB (SSB is only a small fraction of 8-OH-dG).

the BrOI induction of 8-OH-dG here for simplicity. Further, in our model, 8-OH-dG adducts are being repaired by a BER mechanism (labeled OGG1R) that consists of Ogg1 base-excision as an initial step. In some cases the repair process proceeds to produce an intact DNA strand, while in other rare cases, further repair fails and leaves persistent unrepaired SSB (Fig. 7A). In our model, all reactions have fixed rate constants (see Methods). Therefore, according to the mass action law, the increment of SSB per unit time is proportional to the adduct/BER complexes (d[SSB]/dt =k[8-OH-dG.OGG1R]). We also assumed that SSB were formed from 8-OH-dG and not as a result of increased BER activity. We performed a computer simulation based on this model using a MATLAB script (available upon request). KBrO$_3$ at different concentrations was applied at the beginning of the simulated experiment for a short time. The dose-response profile for 8-OH-dG and SSB was computed at a time point after the KBrO$_3$ exposure, shortly before the steady state is reached. As illustrated in Figure 7C, the 8-OH-dG dose dependence appeared to have highly sublinear behavior due to extensive repair. However the SSB dose-response showed close to linear dependence and is completely linear at steady state, when repair processes are completed (not shown). The results from our model have fundamental implications. They demonstrate that even if an early event in carcinogen-

Environmental and Molecular Mutagenesis. DOI 10.1002/em

12   Spassova et al.

esis appears to have a highly sublinear threshold-like behavior, later downstream processes can still exhibit highly linear properties. This is important to consider in reaching conclusions on the toxicity of a chemical based on early genotoxic events.

The observed results for the dose-response patterns for DNA damage and mutation presented here were seen with an oxidative agent that (after biochemical reactions that are not yet fully defined) directly targets DNA. More generally, DNA may be exposed to oxidizing species (such as reactive oxygen species (ROS)), that are generated from a variety of different biological processes. It may not be justified to assume that widely differing biological processes would lead to the same dose-response patterns. Similar linear responses may not occur for agents which, for example, result in generation of ROS due to processes involving overt cellular toxicity and death [Takahashi et al., 1998; Siesky et al., 2002; Eastmond, 2008]. It is also fair to note that other scenarios, for example, effective scavenging of a reactive intermediate at low doses, could create an apparent threshold for the 8-OH-dG generation but would not result in a downstream event's linear dependence on the dose. A pertinent question is then whether dose-response information can be developed to relate the applied dose of a test compound to an appropriate internal indicator of effects resulting from the formation of ROS and other oxidative species. If (at low doses) there is a proportional (linear) relationship between the applied dose of a test agent and exposure of DNA to relevant types of ROS and DNA damaging species in the target cell or organ, our results lend support to an inference of a low-dose linear relationship for the observed DNA damage and mutation. If on the other hand, the relationship between applied dose and reactive species formation is nonlinear (e.g., a threshold-type dose-response), non-linear dose-responses for genotoxic effects might likewise be inferred. Such inferences would be contingent on having sufficient understanding of the biological system to confidently link the observed genotoxic effects to the relevant types of reactive species being produced.

A classification of genotoxic endpoints in terms of biomarkers of exposure vs. biomarkers of effect has been proposed in the literature [Swenberg et al., 2008]. In such a paradigm, DNA adducts such as 8-OH-dG are considered to be biomarkers of exposure, while irreversible mutations are defined as biomarkers of effect. For some environmental chemicals, biomarkers of exposure and effect were found to have different dose-response shapes and background levels, where biomarkers of exposure dose-responses were mostly linear and extrapolated back to zero, while biomarkers of effect had a background level above zero [Swenberg et al., 2008]. However, we did not observe this pattern in our analysis of data on KBrO$_3$.

Traditionally, dose-response studies of toxic chemicals have been used to identify a no-observed-effect-level (NOEL), which is often defined as the highest dose that does not produce a statistically *significant* effect, and a lowest-observed-effect-level (LOEL), the lowest dose that shows a significant response. Frequently, this statistically based analysis is extended further by making a presumption that a threshold occurs at the NOEL or at a level between the NOEL and the LOEL. However, statistical dose-response modeling may not support such a presumption. The analyses here offer examples of high-quality datasets where NOELs were defined, but where statistical modeling indicated the compatibility of the data with a non-threshold, low-dose linear dose-response pattern. Scientifically, this is not a surprising result—any method will lose sensitivity to detect responses as the magnitude of these response declines with decreasing dose.

Generally, a design with more doses in the low dose region, below but close to the LOEL, would improve the power of the analysis to define the dose-response and detect the presence of a rapid change in response that could be indicative of a threshold. Such a design will lead to model fits with high slope indexes, if true thresholds exist. In our analyses, most datasets had a number of doses in the low response region that do improve their ability to discern patterns of response at low dose. When there is a strongly elevated response with a small variance at the LOEL dose, this can serve to provide guidance for further experimentation to define the response relationship at lower doses (see for example, Fig. 4).

In summary, a systematic review of the literature and analysis using dose-response modeling approaches revealed that conclusions regarding the presence of a threshold for the genotoxic effects of KBrO$_3$ are premature and largely unsubstantiated. The datasets implicated in earlier studies as demonstrating a threshold were shown in our analyses to be consistent with low-dose linear models. Furthermore, our kinetic model simulations reveal that even if an upstream genotoxic effect appears to have a dose-response shape consistent with a threshold, downstream endpoints can still exhibit linear dose-response dependence.

Environmental and Molecular Mutagenesis. DOI 10.1002/em

Low-Dose Linearity of Bromate Genotoxicity **13**

STATEMENT OF AUTHOR CONTRIBUTIONS

REFERENCES

Allen JW, Collins BW, Lori A, Afshari AJ, George MH, DeAngelo AB, Fuscoe JC. 2000. Erythrocyte and spermatid micronucleus analyses in mice chronically exposed to potassium bromate in drinking water. Environ Mol Mutagen 36:250–253.

Altham PME. 1978. Two generalizations of the binomial distribution. Applied Statistics 27:162–167.

Arai T, Kelly VP, Minowa O, Noda T, Nishimura S. 2002. High accumulation of oxidative DNA damage, 8-hydroxyguanine, in Mmh/Ogg1 deficient mice by chronic oxidative stress. Carcinogenesis 23:2005–2010.

Arai T, Kelly VP, Komoro K, Minowa O, Noda T, Nishimura S. 2003. Cell proliferation in liver of Mmh/Ogg1-deficient mice enhances mutation frequency because of the presence of 8-hydroxyguanine in DNA. Cancer Res 63:4287–4292.

Awogi T, Murata K, Uejima M, Kuwahara T, Asanami S, Shimono K, Morita T. 1992. Induction of micronucleated reticulocytes by potassium bromate and potassium chromate in Cd-1 male-mice. Mutat Res 278:181–185.

Ballmaier D, Epe B. 1995. Oxidative DNA damage induced by potassium bromate under cell-free conditions and in mammalian cells. Carcinogenesis 16:335–342.

Ballmaier D, Epe B. 2006. DNA damage by bromate: mechanism and consequences. Toxicology 221:166–171.

Bolt HM, Foth H, Hengstler JG, Degen GH. 2004. Carcinogenicity categorization of chemicals-new aspects to be considered in a European perspective. Toxicol Lett 151:29–41.

Chipman JK, Davies JE, Parsons JL, Nair J, O'Neill G, Fawell JK. 1998. DNA oxidation by potassium bromate; a direct mechanism or linked to lipid peroxidation? Toxicology 126:93–102.

Cho DH, Hong JT, Chin K, Cho TS, Lee BM. 1993. Organotropic formation and disappearance of 8-hydroxydeoxyguanosine in the kidney of Sprague-Dawley rats exposed to adriamycin and KBrO3. Cancer Lett 74:141–145.

Crump KS. 2011. Use of threshold and mode of action in risk assessment. Crit Rev Toxicol 41:637–650.

Crump KS, Howe RB. 1985. A review of methods for calculating statistical confidence limits in low dose extrapolation. In: Clayson DB, Krewski D,Munro I, editors. Toxicological Risk Assessment. CRC Press. p 187–203.

DeAngelo AB, George MH, Kilburn SR, Moore TM, Wolf DC. 1998. Carcinogenicity of potassium bromate administered in the drinking water to male B6C3F1 mice and F344/N rats. Toxicol Pathol 26:587–594.

Doak SH, Jenkins GJ, Johnson GE, Quick E, Parry EM, Parry JM. 2007. Mechanistic influences for mutation induction curves after exposure to DNA-reactive carcinogens. Cancer Res 67: 3904–3911.

Eastmond DA. 2008. Evaluating genotoxicity data to identify a mode of action and its application in estimating cancer risk at low doses:

A case study involving carbon tetrachloride. Environ Mol Mutagen 49:132–141.

Ehling UH, Averbeck D, Cerutti PA, Friedman J, Greim H, Kolbye AC, Jr., Mendelsohn ML. 1983. International Commission for Protection against Environmental Mutagens and Carcinogens. ICPEMC publication no. 10. Review of the evidence for the presence or absence of thresholds in the induction of genetic effects by genotoxic chemicals. Mutat Res 123:281–341.

Entezam A, Lokanga AR, Le W, Hoffman G, Usdin K. 2010. Potassium bromate, a potent DNA oxidizing agent, exacerbates germline repeat expansion in a fragile X premutation mouse model. Hum Mutat 31:611–616.

European Commission. Technical Guidance Document in Support of Commission Directive 93/67/EEC on Risk Assessment for New Notified Substances and Commission Regulation (EC) No. 1488/94 on Risk Assessment for Existing Substances. Part 1. 1996.

Frantz CE, Bangerter C, Fultz E, Mayer KM, Vogel JS, Turteltaub KW. 1995. Dose-response studies of MeIQx in rat liver and liver DNA at low doses. Carcinogenesis 16:367–373.

Gocke E, Burgin H, Muller L, Pfister T. 2009. Literature review on the genotoxicity, reproductive toxicity, and carcinogenicity of ethyl methanesulfonate. Toxicol Lett 190:254–265.

Grosovsky AJ, Little JB. 1985. Evidence for linear response for the induction of mutations in human cells by x-ray exposures below 10 rads. Proc Natl Acad Sci U S A 82:2092–2095.

Harrington-Brock K, Collard DD, Chen T. 2003. Bromate induces loss of heterozygosity in the thymidine kinase gene of L5178Y/Tk(+/-)-3.7.2C mouse lymphoma cells. Mutat Res 537:21–28.

Henderson L, Albertini S, Aardema M. 2000. Thresholds in genotoxicity responses. Mutat Res 464:123–128.

IARC. 1999. Some chemicals that cause tumors of the kidney or urinary bladder in rodents and some other substances. [73], 481. IARC Monographs on the Evaluation of Carcinogenic Risks to Humans.

Jansen JG, Vrieling H, van Teijlingen CM, Mohn GR, Tates AD, van Zeeland AA. 1995. Marked differences in the role of O6-alkylguanine in hprt mutagenesis in T-lymphocytes of rats exposed in vivo to ethylmethanesulfonate, N-(2-hydroxyethyl)-N-nitrosourea, or N-ethyl-N-nitrosourea. Cancer Res 55:1875–1882.

Johnson GE, Doak SH, Griffiths SM, Quick EL, Skibinski DO, Zair ZM, Jenkins GJ. 2009. Non-linear dose-response of DNA-reactive genotoxins: recommendations for data analysis. Mutat Res 678:95–100.

Kasai H, Nishimura S, Kurokawa Y, Hayashi Y. 1987. Oral administration of the renal carcinogen, potassium bromate, specifically produces 8-hydroxydeoxyguanosine in rat target organ DNA. Carcinogenesis 8:1959–1961.

Kawanishi S, Murata M. 2006. Mechanism of DNA damage induced by bromate differs from general types of oxidative stress. Toxicology 221:172–178.

Kaya FF, Topaktas M. 2007. Genotoxic effects of potassium bromate on human peripheral lymphocytes in vitro. Mutat Res 626:48–52.

Kurokawa Y, Maekawa A, Takahashi M, Hayashi Y. 1990. Toxicity and carcinogenicity of potassium bromate--a new renal carcinogen. Environ Health Perspect 87:309–335.

Luan Y, Suzuki T, Palanisamy R, Takashima Y, Sakamoto H, Sakuraba M, Koizumi T, Saito M, Matsufuji H, Yamagata K, Yamaguchi T, Hayashi M, Honma M. 2007. Potassium bromate treatment predominantly causes large deletions, but not GC>TA transversion in human cells. Mutat Res 619:113–123.

Lutz WK, Lutz RW. 2009. Statistical model to estimate a threshold dose and its confidence limits for the analysis of sublinear dose-response relationships, exemplified for mutagenicity data. Mutat Res 678:118–122.

Mattioli F, Martelli A, Gosmar M, Garbero C, Manfredi V, Varaldo E, Torre GC, Brambilla G. 2006. DNA fragmentation and DNA repair synthesis induced in rat and human thyroid cells by chemicals carcinogenic to the rat thyroid. Mutat Res 609:146–153.

McDorman KS, Pachkowski BF, Nakamura J, Wolf DC, Swenberg JA. 2005. Oxidative DNA damage from potassium bromate exposure in Long-Evans rats is not enhanced by a mixture of drinking water disinfection by-products. Chem Biol Interact 152:107–117.

Moore MM, Chen T. 2006. Mutagenicity of bromate: implications for cancer risk assessment. Toxicology 221:190–196.

Murata M, Bansho Y, Inoue S, Ito K, Ohnishi S, Midorikawa K, Kawanishi S. 2001. Requirement of glutathione and cysteine in guanine-specific oxidation of DNA by carcinogenic potassium bromate. Chem Res Toxicol 14:678–685.

Nakajima M, Kitazawa M, Oba K, Kitagawa Y, Toyoda Y. 1989. Effect of route of administration in the micronucleus test with potassium bromate. Mutat Res 223:399–402.

Nakajima M, Takeuchi T, Ogino K, Morimoto K. 2002. Lack of direct involvement of 8-hydroxy-2'-deoxyguanosine in hypoxanthine-guanine phosphoribosyltransferase mutagenesis in V79 cells treated with N,N'-bis(2-hydroxyperoxy-2-methoxyethyl)-1,4,5,8-naphthalenetetracarboxyli c-diimide (NP-III) or riboflavin. Jpn J Cancer Res 93:247–252.

Nesslany F, Zennouche N, Simar-Meintieres S, Talahari I, Nkili-Mboui EN, Marzin D. 2007. In vivo Comet assay on isolated kidney cells to distinguish genotoxic carcinogens from epigenetic carcinogens or cytotoxic compounds. Mutat Res 630:28–41.

Parsons JL, Chipman JK. 2000. The role of glutathione in DNA damage by potassium bromate in vitro. Mutagenesis 15:311–316.

Platel A, Nesslany F, Gervais V, Marzin D. 2009. Study of oxidative DNA damage in TK6 human lymphoblastoid cells by use of the in vitro micronucleus test: Determination of No-Observed-Effect Levels. Mutat Res 678:30–37.

Poirier MC, Beland FA. 1994. DNA adduct measurements and tumor incidence during chronic carcinogen exposure in rodents. Environ Health Perspect 102 Suppl 6:161–165.

Pottenger LH, Gollapudi BB. 2009. A case for a new paradigm in genetic toxicology testing. Mutat Res 678:148–151.

Poul JM, Huet S, Godard T, Sanders P. 2004. Lack of genotoxicity of potassium iodate in the alkaline comet assay and in the cytokinesis-block micronucleus test. Comparison to potassium bromate. Food Chem Toxicol 42:203–209.

Priestley CC, Green RM, Fellows MD, Doherty AT, Hodges NJ, O'Donovan MR. 2010. Anomalous genotoxic responses induced in mouse lymphoma L5178Y cells by potassium bromate. Toxicology 267:45–53.

Richardson C, Williams DAAG, Phillips B, Allen JA, Chanter DO. 1989. Analysis of data from in vitro cytogenetic assays. In: Kirkland DJ, editor. Statistical evaluation of mutagenicity data. Cambridge University Press. p 141–154.

Ridout MS. 1994. A response curve that generalizes the rectangular hyperbola. Journal of Applied Statistics 21:143–152.

Robbiano L, Carrozzino R, Puglia CP, Corbu C, Brambilla G. 1999. Correlation between induction of DNA fragmentation and micronuclei formation in kidney cells from rats and humans and tissue-specific carcinogenic activity. Toxicol Appl Pharmacol 161:153–159.

Sai K, Umemura T, Takagi A, Hasegawa R, Kurokawa Y. 1992. The protective role of glutathione, cysteine and vitamin C against oxidative DNA damage induced in rat kidney by potassium bromate. Jpn J Cancer Res 83:45–51.

Sai K, Tyson CA, Thomas DW, Dabbs JE, Hasegawa R, Kurokawa Y. 1994. Oxidative DNA damage induced by potassium bromate in isolated rat renal proximal tubules and renal nuclei. Cancer Lett 87:1–7.

Seager A, Shah UK, Mikhail J, Nelson B, Marquis B, Doak S, Johnson G, Griffiths S, Carmichael P, Scott S, Scott A, Jenkins G. 2012. Pro-oxidant Induced DNA Damage in Human Lymphoblastoid Cells

Siesky AM, Kamendulis LM, Klaunig JE. 2002. Hepatic effects of 2-butoxyethanol in rodents. Toxicol Sci 70:252–260.

Siesky AM, Kamendulis LM, Klaunig JE. 2002. Hepatic effects of 2-butoxyethanol in rodents. Toxicol Sci 70:252–260.

Slob W. 2002. Dose-response modeling of continuous endpoints. Toxicological Sciences 66:298–312.

Speit G, Haupter S, Schutz P, Kreis P. 1999. Comparative evaluation of the genotoxic properties of potassium bromate and potassium superoxide in V79 Chinese hamster cells. Mutat Res 439:213–221.

Swenberg JA, Fryar-Tita E, Jeong YC, Boysen G, Starr T, Walker VE, Albertini RJ. 2008. Biomarkers in toxicology and risk assessment: informing critical dose-response relationships. Chem Res Toxicol 21:253–265.

Takahashi S, Hirose M, Tamano S, Ozaki M, Orita S, Ito T, Takeuchi M, Ochi H, Fukada S, Kasai H, Shirai T. 1998. Immunohistochemical detection of 8-hydroxy-2'-deoxyguanosine in paraffin-embedded sections of rat liver after carbon tetrachloride treatment. Toxicol Pathol 26:247–252.

Umemura T, Kurokawa Y. 2006. Etiology of bromate-induced cancer and possible modes of action-studies in Japan. Toxicology 221:154–157.

Umemura T, Sai K, Takagi A, Hasegawa R, Kurokawa Y. 1995. A possible role for oxidative stress in potassium bromate (KBrO3) carcinogenesis. Carcinogenesis 16:593–597.

Umemura T, Kitamura Y, Kanki K, Maruyama S, Okazaki K, Imazawa T, Nishimura T, Hasegawa R, Nishikawa A, Hirose M. 2004. Dose-related changes of oxidative stress and cell proliferation in kidneys of male and female F344 rats exposed to potassium bromate. Cancer Sci 95:393–398.

Umemura T, Kanki K, Kuroiwa Y, Ishii Y, Okano K, Nohmi T, Nishikawa A, Hirose M. 2006. In vivo mutagenicity and initiation following oxidative DNA lesion in the kidneys of rats given potassium bromate. Cancer Sci 97:829–835.

Yamaguchi T, Wei M, Hagihara N, Omori M, Wanibuchi H, Fukushima S. 2008. Lack of mutagenic and toxic effects of low dose potassium bromate on kidneys in the Big Blue rat. Mutat Res 652:1–11.

Zeiss L, Cardis E, Hemminki K, Schwarz M. 1999. Quantitative estimation and prediction of cancer risk: Review of existing activities. In: Moolgavkar S, Krewski D, Zeiss L, Cardis E, Moller H, editors. Quantitative Estimation and Prediction of Human Cancer Risks. Lyon: International Agency for Research on Cancer. p 11–59.

TABLE AI. DNA Damage by KBrO₃ Exposure Measured by Various Assays

Test	Dose	System level	Route	Species/Organ	Control effect	Max Effect	Reference
8-OH-dG	1 mM +2 mM GSH for 2h	cell free	NA	calf thymus DNA	$4/10^5$ dG	$434/10^5$ dG	[Murata et al., 2001]
8-OH-dG	0.5 to 2 mM for 4 h	in vitro	NA	HL-60 cell culture	$0.3/10^5$ dG	$4.2/10^5$ dG	[Murata et al., 2001]
8-OH-dG	0.5 to 2 mM for 4 h	in vitro	NA	HP-100 cell culture	$0.4/10^5$ dG	$4.1/10^5$ dG	[Murata et al., 2001]
8-OH-dG	15 µM to 1.5 mM with 500 µM GSH	in vitro	NA	calf thymus DNA	$(8 \pm 1)/10^5$ dG	$(91 \pm 33)/10^5$ dG	[Parsons and Chipman, 2000]
8-OH-dG	15 µM to 1.5 mM for 15 min, 37°C with 500 µM GSH	in vitro	NA	calf thymus DNA	$8/10^5$ dG	$90/10^5$ dG	[Chipman et al., 1998]
8-OH-dG	1.5 mM	in vitro	NA	rat kidney epithelial cells (NRK-52E)	$(2.8 \pm 0.3)/10^5$ dG	$(10.2 \pm 0.5)/10^5$ dG	[Parsons and Chipman, 2000]
8-OH-dG	2 and 5 mM for 2 to 4h	in vitro	NA	male F344 rat/renal proximal tubules	$(0.98 \pm 0.22)/10^5$ dG	$(4.8 \pm 0.71)/10^5$ dG	[Sai et al., 1994]
8-OH-dG	10 to 20 mM for 1h	in vitro	NA	V79 Chinese hamster cells	$(0.51 \pm 0.15)/10^5$ dG	$(3.07 \pm 0.43)/10^5$ dG	[Speit et al., 1999]
8-OH-dG	2 g/L for 12 weeks	in vivo	DW	gpt/Ogg1 +/- and gpt/Ogg1 -/- mice/kidney	$0.22/10^5$dG	$45.73/10^5$ dG	[Arai et al., 2002]
8-OH-dG	20 and 100 mg/kg	in vivo	i.p.	Sprague–Dawley rat/kidney	$(1.12 \pm 0.28)/10^5$ dG and $(22.5 \pm 3.1)/10^5$ dG in mitochondria	$(2.3 \pm 0.31)/10^5$ dG and $(35.5 \pm 13.0)/10^5$ dG in mitochondria - 24h after injection	[Chipman et al., 1998]
8-OH-dG	500 mg/kg	in vivo	i.p.	Sprague–Dawley rat/kidney	$5/10^5$ dG	$138/10^5$ dG (27 weeks after injection)	[Cho et al., 1993]
8-OH-dG	500 mg/kg	in vivo	i.p.	Sprague–Dawley rat/liver	$5/10^5$ dG	$42/10^5$ dG (24 weeks after injection)	[Cho et al., 1993]
8-OH-dG	0.5 g/L for more than two generations	in vivo	DW	FX PM mice/oocytes	NA	3-fold increase over control (measured with antibody)	[Entezam et al., 2010]
8-OH-dG	400 mg/kg	in vivo	i.g.	F344 rats/kidney	$1.3/10^5$ dG	$5.8/10^5$ dG (24h)	[Kasai et al., 1987]
8-OH-dG	400 mg/kg	in vivo	i.g.	F344 rats/liver	$1.5/10^5$ dG	$2.44/10^5$ dG	[Kasai et al., 1987]
8-OH-dG	0.4 g/L for 3 weeks	in vivo	DW	Long-Evans rats/kidney	not detected	$0.162/10^5$ dG	[McDorman et al., 2005]
8-OH-dG	20 and 80 mg/kg	in vivo	i.p.	male F344 rats/kidney	$(2.7 \pm 0.67)/10^5$	$(8.7 \pm 1.2)/10^5$ dG at 48 h	[Sai et al., 1992]
8-OH-dG	60 to 500 ppm for up to 13 weeks	in vivo	DW	gpt delta rats/kidney	$(0.28 \pm 0.06)/10^5$ dG	$(0.88 \pm 0.10)/10^5$ dG at 5 weeks	[Umemura et al., 2006]
8-OH-dG	15 to 500 ppm for 4 weeks	in vivo	DW	female F344 rats/kidney	$(0.25 \pm 0.05)/10^5$ dG	$(0.70 \pm 0.16)/10^5$ dG	[Umemura et al., 2004]
8-OH-dG	15 to 500 ppm for 4 weeks	in vivo	DW	male F344 rats/kidney	$(0.31 \pm 0.06)/10^5$ dG	$(0.71 \pm 0.21)/10^5$ dG	[Umemura et al., 2004]
8-OH-dG	300 mg/kg i.g intubation and 80 mg/kg i.p. injection - test at 48 h	in vivo	intub; i.p.	female F344 rats	$0.33/10^5$ dG	i.g. $0.87/10^5$ dG i.p. $0.76/10^5$ dG	[Umemura et al., 2004]
8-OH-dG	100 to 400 mg/kg - test at 48 h	in vivo	i.g.	female F344 rats/kidneys	$(0.37 \pm 0.10)/10^5$ dG	$(1.54 \pm 0.15)/10^5$ dG	[Umemura et al., 1995]
8-OH-dG	100 to 400 mg/kg - test at 48 h	in vivo	i.g.	female F344 rats/liver	$0.49/10^5$ dG	$0.56/10^5$ dG (not significantly different from control)	[Umemura et al., 1995]

TABLE AI. DNA Damage by $KBrO_3$ Exposure Measured by Various Assays (Continued)

Test	Dose	System level	Route	Species/Organ	Control effect	Max Effect	Reference
8-OH-dG	500 ppm in drinking water	in vivo	DW	rats/kidney	$0.8/10^5$ dG	$1.84/10^5$ dG (3 weeks treatment)	[Umemura et al., 1995]
8-OH-dG	0.02 to 500 ppm for 16 weeks (0.53 to 13,774 µg/rat/day)	in vivo	DW	Big Blue rats/kidney	$(0.75 \pm 0.18)/10^5$ dG	$(1.4 \pm 0.22)/10^5$ dG	[Yamaguchi et al., 2008]
8-OH-dG	5 mM for 15 min and 1h	in situ	NA	Sprague–Dawley rat/kidney	$(2.3 \pm 1.1)/10^5$ dG and $(21.0 \pm 8.9)/10^5$ dG for mitochondria	$(3.56 \pm 0.88)/10^5$ dG and $(25.7 \pm 13.9)/10^5$ dG for mitochondria	[Chipman et al., 1998]
8-OH-dG	15 µM to 1.5 mM for 15 min, 37°C	in vitro	NA	calf thymus DNA	$8/10^5$ dG (500 mM GSH)	$90/10^5$ dG (500 µM GSH)	[Chipman et al., 1998]
8-OH-dG	2 g/L for 12 weeks	in vivo	DW	gpt/Ogg1 +/- and gpt/Ogg1 -/- mice/liver	$1.64/10^5$ dG	$11.35/10^5$ dG	[Arai et al., 2003]
COM	0.625 to 10 mM for 3h	in vitro	NA	CHO cells	OTM = 1.15; when highly damaged cells excluded, OTM = 0.72 ± 0.15	OTM = 23.8; when highly damaged cells excluded OTM = 16.42 ± 1.41	[Poul et al., 2004]
COM	0.5 to 5 mM for 4h	in vitro	NA	human lymphoblastoid TK6 cells	TL: 9.7 µm	TL: 37.2 µm	[Luan et al., 2007]
COM	2.5 to 5 mM for 20h	in vitro	NA	primary cultures of human thyroid cells	TL: (1.9 ± 0.4) µm	TL: (9.9 ± 3.5) µm	[Mattioli et al.,2006]
COM	5 mM	in vitro	NA	human white blood cells		7% tail increase	[Parsons and Chipman, 2000]
COM	1 p.o. at 160 mg/kg and 3 p.o. at 107 mg/kg	in vivo	oral	Sprague–Dawley male albino rats/kidney	TL: (3.2 ± 10.8) µm	TL: (4.7 ± 12.1) µm and (16.9 ± 23.2) µm	[Robbiano et al., 1999]
COM	0.56 to 1.8 mM	in vitro	NA	primary cultures of human kidney cells	TL: (6.6 ± 2.2) µm; TM: 712±231	TL: (46.5 ± 19.5) µm; TM: 3569±1481	[Robbiano et al., 1999]
COM	0.56 to 1.8 mM	in vitro	NA	primary cultures of Sprague–Dawley male albino rat kidney cells	TL: (3.6 ± 3.2) µm; TM: 339±301	TL: (41.1 ± 18.4) µm; TM: 3267±1601	[Robbiano et al., 1999]
COM	1 mM to 20 mM	in vitro	NA	V79 Chinese hamster cells	TM: 0.1	TM: 4.15	[Speit et al., 1999]
COM	200 and 400 mg/kg	in vitro	NA	kidney cells from OFA Sprague–Dawley male rats	Median OTM 0.89	Median OTM 1.22	[Nesslany et al., 2007]
COM	160 mg/kg	in vivo	oral	Male Sprague–Dawley rats/thyroid	TL: (1.8 ± 0.7) µm	TL: (19.3 ± 3.1) µm	[Mattioli et al., 2006]
COM	160 mg/kg	in vivo	oral	Male Sprague–Dawley rats/liver	TL: (2.5 ± 0.4) µm	TL: (4.5 ± 0.8) µm	[Mattioli et al., 2006]
COM	160 mg/kg	in vivo	oral	Male Sprague–Dawley rats/kidney	TL: (2.2 ± 0.6) µm	TL: (19.1 ± 1.3) µm	[Mattioli et al., 2006]
MF	0.06 to 3 mM for 4 h	in vitro	NA	L5178Y/Tk$^{+/-}$ mouse lymphoma cells	$111/10^6$ surviving cells	$1483/10^6$ surviving cells	[Harrington-Brock et al., 2003]
MF(TK,HPRT)	0.5 to 4 mM for 3h	in vitro	NA	mouse lymphoma L5178Y cells	$90/10^6$ tk; $1.5/10^6$ hprt	$4127/10^6$ tk; $16.7/10^6$ hprt	[Priestley et al., 2010]

TABLE AI. DNA Damage by KBrO$_3$ Exposure Measured by Various Assays (Continued)

Test	Dose	System level	Route	Species/Organ	Control effect	Max Effect	Reference
MF (TK)	0.5 to 5 mM for 4hr	in vitro	NA	human lymphoblastoid TK6 cells	2.76/10^6	63.5/10^6	[Luan et al., 2007]
MF (HPRT)	5 mM to 20 mM for 1h	in vitro	NA	V79 Chinese hamster cells	4/10^6	72/10^6	[Speit et al., 1999]
MF (gtp)	2 g/L for 12 weeks	in vivo	DW	gpt/Ogg1 +/- and gpt/Ogg1 -/- mice/liver	(11.9 ± 6.10)/10^6 after liver regeneration	(35.5 ± 15.7)/10^6 after liver regeneration	[Arai et al., 2003]
MF (gtp)	2 g/L for 12 weeks	in vivo	DW	gpt/Ogg1 +/- and gpt/Ogg1 -/- mice/kidney	(2.9 ± 1.0)/10^6	(28.8 ± 6.5)/10^6	[Arai et al., 2002]
MF (lacI)	0.02 to 500 ppm for 16 weeks (0.53 to 13774 μg/rat/day)	in vivo	DW	Big Blue rats/kidney	(22.4 ± 12.2)/10^6	(61.9 ± 24.0)/10^6	[Yamaguchi et al., 2008]
MF (Spi-)	60 to 500 ppm for up to 13 weeks	in vivo	DW	gpt delta rats/kidney	(0.28 ± 0.16)/10^5	(0.99 ± 0.45)/10^5	[Umemura and Kurokawa, 2006]
MN	0.625 to 10 mM for 3h	in vitro	NA	CHO cells	2.2% MNBN	34.2% MNBN	[Poul et al., 2004]
MN	0.5 to 4 mM for 3h	in vitro	NA	mouse lymphoma L5178Y cells	0.40%	6%	[Priestley et al., 2010]
MN	0.5 to 5 mM for 4h	in vitro	NA	human lymphoblastoid TK6 cells	3.5/1000	83.5/1000	[Luan et al., 2007]
MN	6.25 μM to 1 mM	in vitro	NA	TK6 human lymphoblastoid cells	0.01	0.067	[Platel et al., 2009]
MN	400 to 550 μg/ml for 24 and 48h	in vitro	NA	human peripheral blood lymphocytes	(0.18 ± 0.02)/100	(1.1 ± 0.18)/100 (at 500 μg/ml)	[Kaya and Topaktas, 2007]
MN	0.56 to 1.8 mM	in vitro	NA	primary cultures of human kidney cells	2.11/1000	9.47/1000	[Robbiano et al., 1999]
MN	0.56 to 1.8 mM	in vitro	NA	primary cultures of Sprague–Dawley male albino rat kidney cells	(1.77 ± 1.04)/1000	(11.4 ± 4.29)/1000	[Robbiano et al., 1999]
MN	0.08-0.8 g/L for 8,78 weeks	in vivo	DW	B6C3F1 mice/normochromatic erythrocyte	(1.40 ± 0.02)/1000	(6.1 ± 0.08)/1000	[Allen et al., 2000]
MN	18.8 to212 mg/kg	in vivo	i.p.	CD-1 male mice/peripheral blood reticulocytes (PB-RETs)	(1.6 ± 0.9)/1000	(23.4 ± 3.6)/1000	[Awogi et al., 1992]
MN	37.5 to 300 mg/kg	in vivo	i.g.	MS/Ae and CD-1 mice/polychromatic erythrocytes	(0.23 ± 0.22)/100	(2.28 ± 1.23)/100	[Nakajima et al., 1989]
MN	18.8 to 150 mg/kg	in vivo	i.p.	MS/Ae and CD-1 mice/polychromatic erythrocytes	(0.30+0.14)/100	(3.78 ± 0.97)/100	[Nakajima et al., 1989]
MN	160 mg/kg p.o.	in vivo	oral	Sprague–Dawley male albino rats/kidney	(0.73 ± 0.49)/1000	(2.81 ± 1.18)/1000	[Robbiano et al., 1999]
REL	0.1 to 1 mM for 15 min, 37°C	cell free	NA	bacteriophage PM2 DNA	0.1 modifications/10^4 bp (2 mM GSH)	1.25 modifications/10^4 bp (2 mM GSH)	[Ballmaier and Epe, 2006]

8-OHdG, 8-hydroxy-2'-deoxyguanosine (includes its tautomer 8-oxo-2'-deoxyguanosine); Gtp, mutations affecting the gtp gene; i.g, single intragastric administrations; i.p., intraperitoneal injection; DW, drinking water; COM, comet assay; MN, micronucleus assay; MF, mutant frequency; HPRT, mutations at the HPRT locus; REL, relaxation assay; Spi, mutations affecting the Spi gene; TK, thymidine kinase (TK) gene mutation assay; LacI, mutation frequencies of LacI gene; (O)TM, (Olive) tail moment; TL, tail length.